Prediction of Static Recrystallisation during Extrusion of Aluminium Alloy AA2024

Zhi Peng and Terry Sheppard
School of Dec Bournemouth University
S105, 12 Christchurch Road, Bournemouth, U.K.
Email: Zpeng@bournemouth.ac.uk

Keywords
Extrusion, Simulation, recrystallisation, aluminium

Abstract

Extrusions experience large deformations at discontinuities when they traverse the die land, leading to considerable modifications to the average deformation parameters when compared to the remainder of the extrusion. The distribution of structure is therefore greatly inhomogeneous. Reference to both empirical and physical models of the recrystallisation process indicate that nucleation and growth will differ at these locations in those alloys that are usually solution treated and aged subsequent to the deformation process. In the work presented, a physical model based on dislocation density, subgrain size and misorientation is integrated into the commercial FEM codes, FORGE2® and FORGE3® to study the microstructure changes. Axi-symmetrical and shape extrusion are presented as examples. The evolution of the substructure influencing static recrystallisation is studied. The metallurgical behaviour of axi-symmetric extrusion and that of shape extrusion are compared. The predicted results show good agreement with experimental measurement.

Introduction

Aluminium and its alloys have good working characteristics in all the conventional metallurgical processes, such as rolling and extrusion. Since a range of commercial Al-Cu-Mg alloys has been developed, AA2024 and AA2014 are now the most widely used alloys of this systmen. The composition of AA2024 is shown below in table 1.

Table 1. Typical Composition of AA2024

Alloy	Cu	Si	Mn	Mg	Fe
2024	4.5	-	0.6	1.5	0.2

In order to achieve the optimum mechanical properties in AA2024, it is usually necessary to solution heat treat and age the wrought product. Apart from the heavily worked outer region, the structure can be fully recrystallised, fibrous, or a combination of both. The structures may be classified into three main typical types as shown in Fig. 1. Frequently the structure was a combination of one or more of these types (Sheppard 1993).

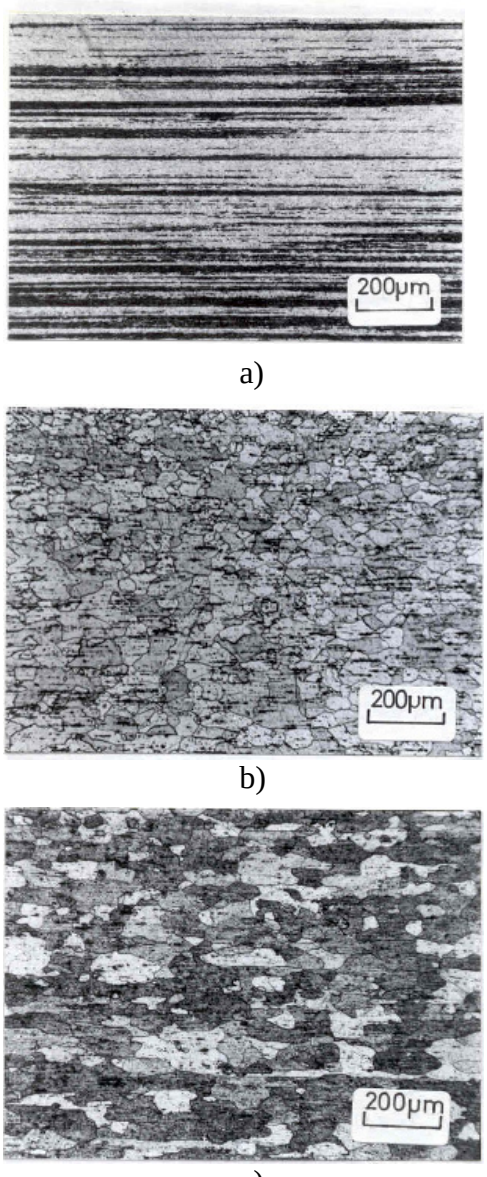

Figures 1: Optical micrographs of typical structures

Micrograph (a) is of a typical fibrous structure with very long grains aligned in the extrusion direction. The similarity between this structure, formed at high temperatures, and that produced by a large reduction at

Proceedings 15th European Simulation Symposium
Alexander Verbraeck, Vlatka Hlupic (Eds.)

ISBN 3-936150-28-1 (book) / 3-936150-29-X (CD)

low temperatures, prompted much of the current interest in hot working and dynamic recovery.

In (b) an elongated structure can still be detected but recrystallization has occurred. Some of the recrystallized grains have their largest axis in the extrusion direction. The extent of the elongation is exaggerated by the aligned precipitates, they tend to make the grains appear longer than they are in reality. The fibrous structure occurs over a wide range of flow stress in the manganese-bearing alloy.

In (c) a fully recrystallized structure is seen. The only indication of the extensive deformation that has been used is the preferential orientation of the precipitates, which lie in the direction of extrusion. These precipitates appear to be much larger than those observed under the electron microscope. Two reasons for this may be given. One is the exaggeration of the size caused by the etchant. The other is that such large precipitate would be unlikely to thin down with the bulk matrix during the preparation of the thin foils.

In the extrusion of AA2024, due to the stored deformation energy within the extrudate, static recrystallisation ususlly occurs and extends to 100% of the material in some cases. The production of coarse grains is unbeneficial in subsequent heat treatment as it causes a reduction in mechanical property. Damage tolerance, fatigue crack propagation or corrosion, which are three very import technical indexes required by the aerospace industry, are significantly affected by the recrystallised grain size and the volume fraction recrystallised. It has also been shown that this problem becomes greater as the complexity of section shape increases.

Hense, knowledge of the variation of the recrystalised grain size with time and space assists optimisation of the extrusion process.

Metallurgical Model

By empirical and physical means, a modest degree of prediction of microstructure can now be achieved. Excellent reviews on modelling of static recrystallisation (SRX) have been given by Gottstein et al. (Gottstein et al. 1999; Marx et al. 2000) and by Shercliff and Lovatt (Shercliff 1999). Some of the modelling work has been achieved in the field of hot rolling (Chen et al. 1992), and recently in the field of hot extrusion by Duan and Sheppard (Duan and Sheppard 2002). Some models introduce many tuning parameters, especially for the physically based models. These parameters depend mainly on the material. To estimate their real values, specific and numerous experiments would be required. Recently, the inverse method combined with FEM has been adopted to tune the values of these parameters. The FEM is run iteratively until the appropriate value is found to match the experimental measurement. Duan and Sheppard (Duan and Sheppard 2003) have used the inverse method to give the parameters for alloy 5083 and 2014.

The relationship between the volume fraction recrystallised (Xv) and the holding time (t) is generally represented by the Johnson-Mehl-Avrami –Kolmogorov equation (JMAK), which predicts the relationship between the volume fraction recrystallised (Xv) and the holding time (t) and is generally represented as:

$$Xv = 1 - \exp\{-0.693(\frac{t}{t_{50}})^{k}\} \qquad (1)$$

where t is annealing time, k is the Avrami exponent with a commonly reported value of 2, t_{50} is the time to 50% recrystallisation. For the calculation of t_{50}, the physical model is commonly regarded as revealing the mechanics driving the transformation. Previous studies (Furu et al. 1999) have shown that the physical models describe the experimental results well for uniform processing conditions. The model was also successfully applied to tests in which the strain rate was increased (when microstructure transients were not observed). Recently, Sheppard and Duan (Duan and Sheppard 2002) have confirmed that the physical model will give better computed results than the empirical model in the simulation of aluminium extrusion. Only the physical model proposed by Furu and Zhu et al (Zhu and Furu 2000) has been used in this study.

In equation (9), t_{50} is calculated based on the stored energy (P_D) and the density of recrystallisation nuclei (N_V) (Furu 1999).

$$t_{50} = \frac{C}{M_{GB} P_D}(\frac{1}{N_V})^{1/3} \qquad (2)$$

where C / M_{GB} is a further calibration constant. N_V is defined as:

$$N_V = (C_d / \delta^2) S_V(\varepsilon) \qquad (3)$$

where C_d is a further calibration constant, δ is the subgrain size, S_V is the grain boundary area per unit volume

$$S_V(\varepsilon) = (2 / d_0)[\exp(\varepsilon) + \exp(-\varepsilon) + 1] \qquad (4)$$

The stored energy P_D is approximated by

$$P_D = \frac{Gb^2}{10}[\rho_i(1 - Ln(10b\rho_i^{1/2})) + \frac{2\theta}{b\delta}(1 + Ln(\frac{\theta_c}{\theta}))]$$

……..(5)

where G is the shear modulus, b is the burgers vector, ρ_i is the internal dislocation density, θ is the misorientation and θ_c is the critical misorientation for a high angle boundary (~15^0).

The evolution of δ, ρ_i and θ has been explicitly expressed in differential form based on the most classical theories of work hardening and dynamic recovery.

$$d\delta = \frac{\delta}{\varepsilon_\delta \delta_{ss}}(\delta_{ss} - \delta)d\varepsilon \qquad (6)$$

$$d\theta = \frac{1}{\varepsilon_\theta}(\theta_{ss} - \theta)d\varepsilon \qquad (7)$$

$$d\rho_r = d\rho_r^+ + d\rho_r^- = (C_1\rho_r^{1/2} - C_2\frac{\sigma_f}{Z}\rho_r)d\varepsilon \qquad (8)$$

where δ_{ss} and θ_{ss} are the subgrain size and misorientation at steady state deformation. ε_δ and ε_θ are characteristic strains, ρ_r is random dislocation density, C_1 and C_2 are constants. The internal dislocation density consists of two parts, ρ_r and ρ_g (the geometrical necessary dislocation density).

$$\rho_i = \rho_r + \rho_g \qquad (9)$$

$$\rho_g = \frac{1}{b}(\frac{1}{R_g} - \frac{\theta}{\delta}) \qquad (10)$$

where ρ_i is the internal dislocation density, $1/R_g$ is the local lattice curvature.

For site-saturated nucleation, the recrystallised grain size is simply calculated from nucleation density as

$$d_{rex} = DN_V^{-1/3} \qquad (11)$$

where D is a constant.

Experimental Procedure

The material used for the current research work was supplied by Alcan Labs, Banbury, in the form of semi continuous logs of 86mm diameter. The billets were homogenised prior to extrusion at $500^0 C$ for 24 hours and furnace cooled. The homogenised billets were then machined to a diameter of 73mm and cut into billets of required length of 95mm. Specimens for mechanical testing, for heat treatment and for optical and electron microscopy were cut from a position one third along the extrudate in order to ensure steady state conditions. Specimens were also taken along the length of the extrudate to determine the range of properties. The final 60cm of the extrusion was never used since this region remained unquenched. Transverse and longitudinal sections of 2-3 mm thickness were cut from the extrudates and grounded to a thickness of 0.25 – 0.3 mm on the silicon carbide paper. 3 mm discs were punched from these sections and electropolished in a commercial struers jet thinner. The solution was maintained at -$30^0 C$ and a potential of 13 volts was applied between the discs and solution (Sheppard 1993).

FEM Simulation Setting

The FEM programs, FORGE2® and FORGE3® are used in the present study. It is a process simulation tool based on the Finite Element Method. The hyperbolic sine function was combined into the FEM to describe the material behaviour. The constitutive equation can be written as:

$$\overline{\sigma} = \frac{1}{\alpha}Ln[(\frac{Z}{A})^{\frac{1}{n}} + [(\frac{Z}{A})^{\frac{2}{n}} + 1]^{\frac{1}{2}}] \qquad (12)$$

where α, A, n are temperature independent constants, Z is the Zener-Hollomon parameter,

$$Z = \dot{\varepsilon}\exp(\frac{\Delta H}{RT}) \qquad (13)$$

where $\dot{\varepsilon}$ is the strain rate, ΔH is the activation energy and T is the temperature (Sheppard 1993).
For aluminium alloy AA2024, ΔH =148880KJ/mol, α =0.016 m^2/MN, n=4.27, LnA= 19.6.

Two-dimensional simulation results

An axi-symmetrical simulation was performed by Forge2® to check the effect of the metallurgical model. The simulation settings are shown in Table 2. The container temperature is 50 K lower than the initial billet temperature. The friction coefficients between the billet and the die and between the billet and the ram are set as 0.3. The extrusion ratios is 40.

The predicted recrystallized grain size and the subgrain size corresponded well with the experimental measurement along the transverse direction, as can be seen from figure2,3. It is easy to see from figure 2 that the difference between the calculated subgrain size at the centre (2.27 μm) and the experimental measurement (2.22 μm) is no more than 1.0%. At the edge of the extrudate, the predicted subgrain size is 2.52 μm, which is just 0.3% higher than the experimental result (2.45 μm). It is clear from figure 2 that the predicted subgrain size increases as the temperature rises along the tranverse direction of the extrudate. This phenomenon is the same as that observed previously (Sheppard 1993). From figure 3, the recrystallized grain size shows a sharp decrease at the surface of the extrudate, and it is easy to see the

Table 2. Two-dimensional Simulations

Extrusion mode	Material used	Billet temperature (Kelvin)	Die fillet radius	Ram speed (mm/s)	Friction coefficient
Direct	AA2024	683	0.5	3.0	1.0

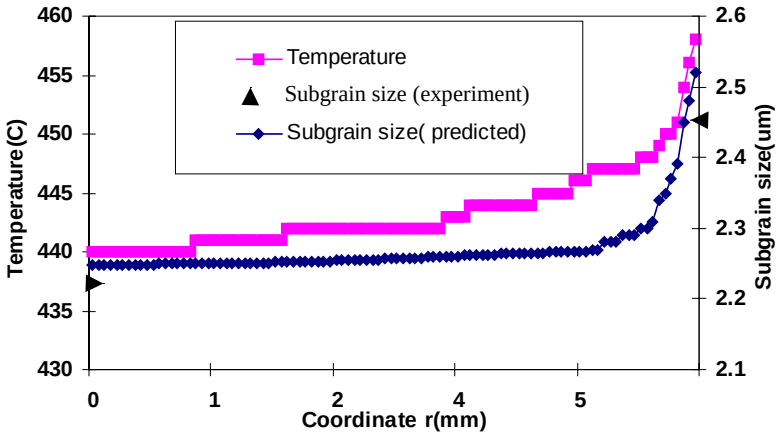

Figure 2. Subgrain Size and Temperature

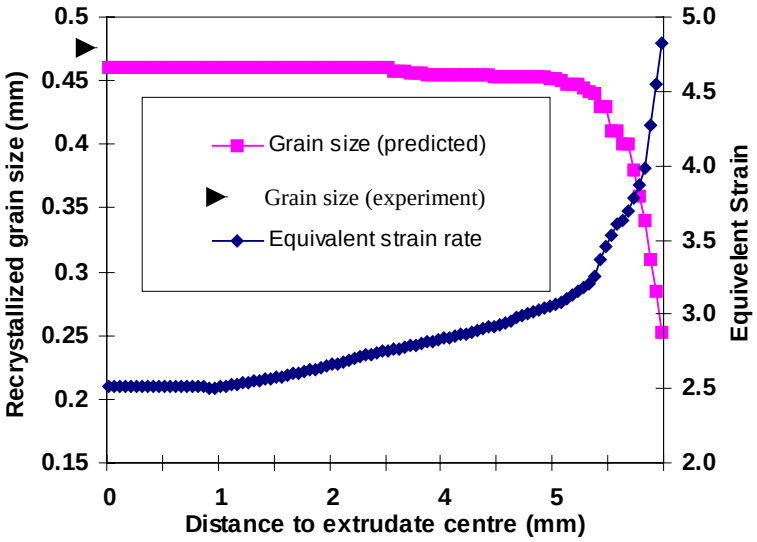

Figure 3. Recrystallized Grain Size and Equivalent Strain

grain size is in inverse proportion to the equivalent strain. This has also been observed before by Vierod and many others (Sellars and Zhu 2000). The predicted value is 0.455mm, which is 3.2% lower than the experimental results.

For the predicted result of volume fraction recrystallisation, the simulation give a slightly rising prediction along the extrudate surface, as can been seen from figure 4. This phenomenon has been observed in the previous experiment. It should be noticed that the experimental measurement, which is 27.37%, is an average value along the extrudate. It is difficult to compare the variation of the predicted Xv with the averaged experimental measurement. The method used in this study to solve this problem was to find a point, whose Y coordinate gave the best corresponce to the experimental result in the given curve. At the same time, the X coordinate of this point and the running step of the simulation were picked out, and the predicted Xv of the other simulations were obtained from the point with the same coordinate and at the same time step. Because the rise of Xv during the extrusion is small, the value picked out from the point can be regarded as the mean value along the extrudate.

Three dimensional simulation results

In this paper, two types of shape extrusion, the T shape and the U shape, are studied. The dimensions of these two shapes are shown in figure. 5. The simulation runs are shown in table 3.

Table 3 Shape Section Extrusion

runs	Type	ratio	temp (Kelvin)	speed (mm/s)
1	T	40	623	7
2	U	40	623	7

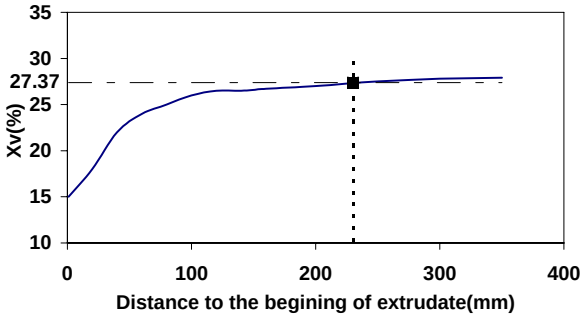

Figure 4. Predicted Xv along Extrudate Surface and the Selected Point

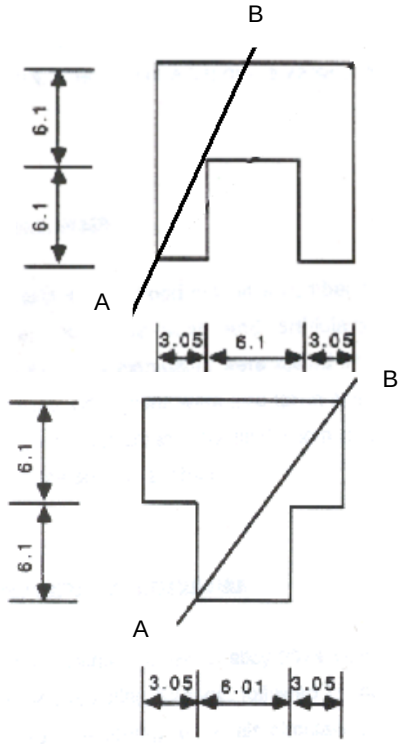

Figure. 5 Dimensions of Shape Sections

Compared with the axi-symmetrical extrusion, the material flow is inhomogeneous in shaped extrusion. The flow patterns corresponding to the extrusion of rod and shape sections are shown in figure 6. The shape sections are cut from face AB, as shown in figure 5. It can be seen from figure 6 that though the general flow pattern remains similar to that in rod extrusion, a certain amount of asymmetry about the billet axis can be envisaged, especially in the regions close to the die shoulders (dead metal zone). The asymmetrical material flow pattern has an important influence on the metallurgical behaviour during shape extrusion, which will be discussed below.

The recrystallised grain size and the equivalent strain distribution of the two sections are shown in figures 7-10. As can be seen in the figures 8 and 10, unlike the axi-symmetrical extrusion, the recrystallised grain size around the periphery of the shape section is inhomogeneous. The inverse relationship between the recrystallised grain size and the equivalent strain also exists in shape sections. In the area where sharp deformation occurs, the recrystallised grain size is smaller than the other areas.

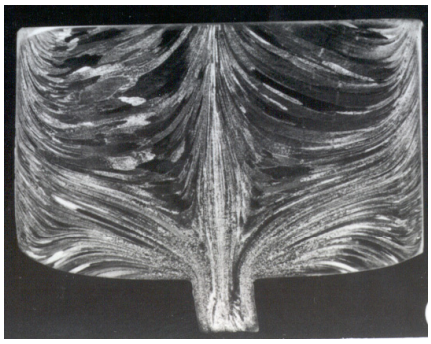

a) Rod

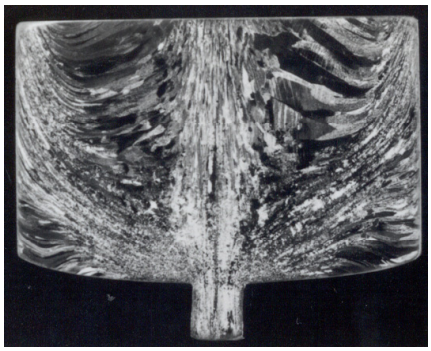

b) U shape

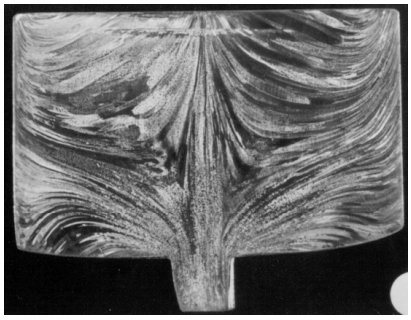

c) Tshape

Figure 6 Macrosections of Partially Extruded Billets

Table 4 Fraction Recrystallised Factors of the T Shape Extrusion

Point	Equivalent strain	Xv	Point	Equivalent strain	Xv
1	2.1	0.61	8	3.19	0.7
2	3.37	0.6	9	3.36	0.78
3	3.04	0.65	10	3.38	0.65
4	2.97	0.60	11	3.40	0.72
5	4.06	0.69	12	3.17	0.62
6	4.15	0.82	13	3.4	0.66
7	4.81	0.72			

Table 5 Fraction Recrystallised Factors of the U Shape Extrusion

Point	Equivalent strain	Xv	Point	Equivalent Strain	Xv
1	2.62	0.95	6	4.19	0.99
2	3.42	0.99	7	4.92	0.99
3	4.62	0.99	8	3.9.3	0.99
4	4.4	0.99	9	5.37	0.99

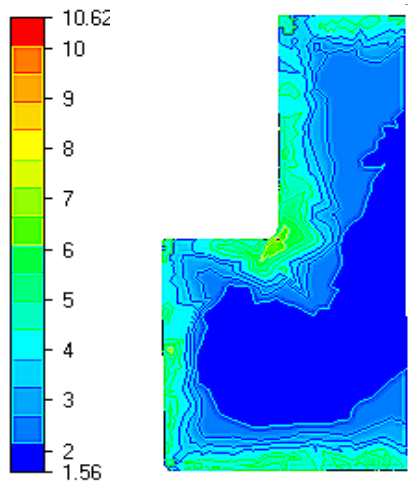

Figure. 7 Equivalent Strain Distribution

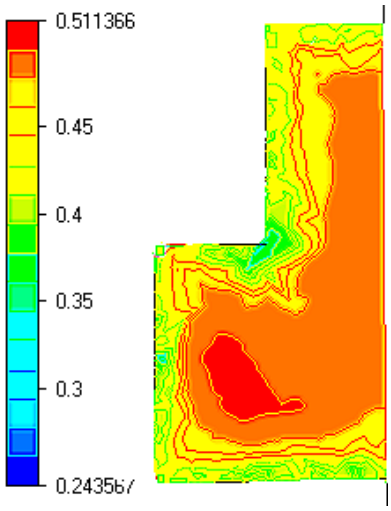

Figure. 8 Recrystallised Grain Size

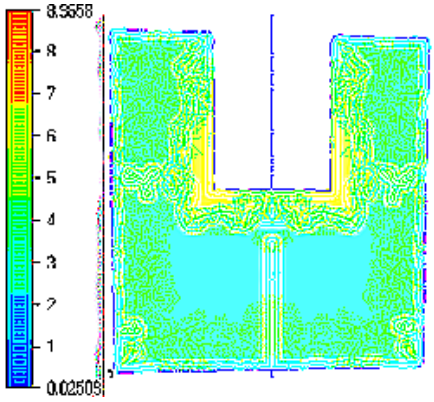

Figure. 9 Equivalent Strain Distribution

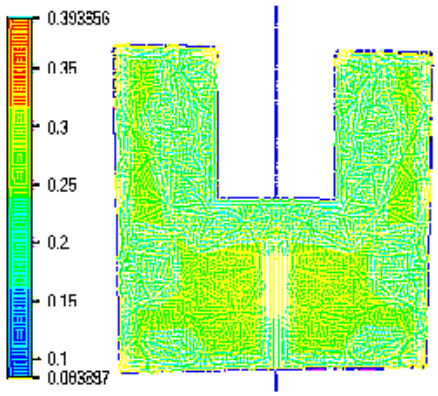

Figure. 10 Recrystallised Grain Size

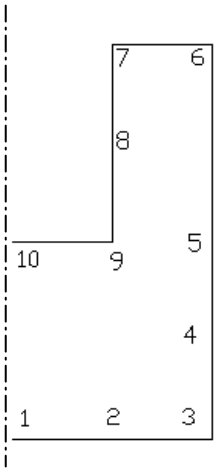

(a) U shape

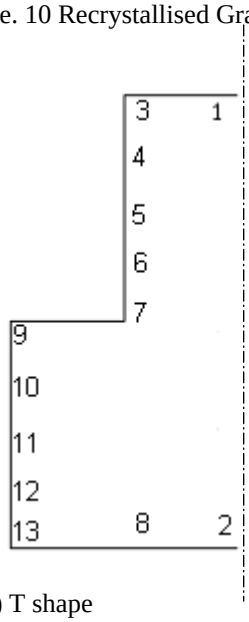

b) T shape

Figure 11 Position of the Points in Table 4

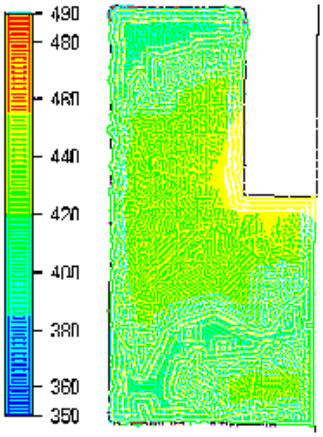

(a) U shape

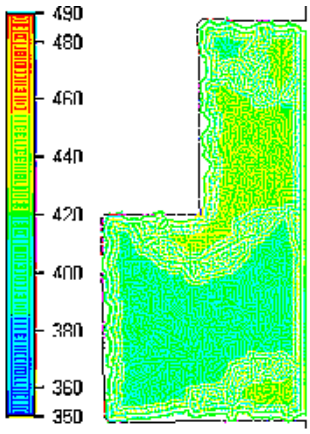

(b) T shape

Figure 12 Temperature Distribution

The predicted fraction recrystllised factors at the periphery of the two sections are shown in table 4 and table 5 respectively. The positions of the points used in these tables are shown in figure 11. For shaped sections, estimation of the depth of the recrystallised layer was difficult in previously experiments, since the layer was no longer uniform. With FEM simulation, the distribution of the volume fraction recrystallised factors can be predicted and extracted more easily. It has been found that both in previous experiments and FEM simulations that the recrystallised layer was thicker for more complex sections due to larger

temperature rise. As can be seen in table 4 and 5, at the positions where the deformation is more complex, that is, where the strain and the temperature are higher, the volume fraction recrystallised is also higher. The temperature distribution across the shape extrudates is shown in figure 12. It can be seen that at the place where a sharper deformation occurs, the temperature and the volume fraction recrystallised are higher, but at the same time, it should be noted that at the corners, the temperature is lower than the other places. It is easy to see that the U shape section experiences larger deformation than the T shape. After the shape sections been extruded to the same diatance, the temperature rise and the equivalent strain of the U shape are higher than that of the T shape. The volume fraction recrystallised is also much more significant in the U shape than the T shape.

It can be seen from the discussion above that, due to the different flow pattern to axi-symmetrical extrusion, the recrystallised grain size and the volume fraction recrystallised factor are inhomogeneous around the periphery of the sections.

Conclusion

FEM simulation is effective in predicting the metallurgical behaviour happened during extrusion. The calculated recrystallised grain size, the subgrain size and the volume fraction recrystallised in this study are in reasonable agreement with the previous experimental resutls.

Reference

Aretz, H.; R. Luce.; M. Wolske.; R. Kopp.; M. Goerdeler; V. Marx.; G. Pomana.; and G. Gottstein. 2000. "Integration of physically based models into FEM and application in simulation of metal forming processes." *Modelling and Simulation in Materials Science and Engineering*, 8 (Nov), 881-891.

Chen, B. K.; Thomson, P. F.; and Choi, S. K. 1992. "Computer modelling of microstructure during hot flat rolling of aluminium." *Materials Science and Technology*, 8 (Jan), 72-77.

Duan, X. and T. Sheppard, 2002. "Influence of forming parameters on static recrystallization behaviour during hot rolling aluminium alloy 5083." *Modelling and simulation in materials science and engineering*. 10, 363-390.

Duan, X. and T. Sheppard. 2002. "Simulation of substructural strengthening in hot flat rolling." *Materials processing Technology*, 125-126, (Sep), 179-187.

Duan, X. and T. Sheppard. 2003. "Computation of substructural strengthening by the integration of metallurgical models into the finite element code." *Computational Materials Science*, 27, 250-258.

Furu, T.; H. R. Shercliff; C. M. Sellars; and M. F. Ashby. 1996. "Physically-based modelling of strength, microstructure and recrystallisation during thermomechanical processing of Al-Mg alloys." *Mater. Sci. Forum*. 217-222, 453-458.

Furu, T.; H. R. Shercliff; G. J. Baxter.; and C. M. Sellars. 1999. "Influence of transient deformation conditions on recrystallization during thermomechanical processing of an Al-1% Mg alloy." *Acta. Mater.* 47, 2377-2388.

Johnson, W. and H. Kudo. 1962. *The mechanics of metal extrusion*, Manchester University Press, Manchester, 60-67.

Marx, V.; F. R. Reher.; and G. Gottstein. 1999. **"**Simulation of primary recrystallization using a modified three-dimensional cellular automaton." *Acta Materialia*, 47, 1219-1230

McLaren, A. J. 1994, Phd Thesis, University of Sheffield.

Sellars, C. M. and Q. Zhu. 2000. "Microstructural modelling of aluminium alloys." Microstructure and Processing, 280, 1-7.

Sheppard, T. 1993. "Extrusion processing parameter-mechanical property correlations in rapidly solidified Al-6·7Fe-5·9Ce and Al-6·2Fe-5·9Ce-1·63Si (wt-%) alloy powders*" Material Science and Technology*, 9(May), 430-440.

Shercliff, H. R. and A. M. Lovatt. 1999. "Modelling of microstructure evolution in hot deformation." *Phil. Tran. R. Soc. Lond. A*, 357 1621-1633.

AUTHOR BIOGRAPHIES

Professor Terry Sheppard has spend his working life in the metals industry. He occupied senior posts with Loewy Engineering and Tube Investment before moving to Imperial College, London where he developed research in the metal forming area for thirty years and was Professor of Industrial Metallurgy. He retired from Imperial College in 1991 and since then he has developed his consultancy work, especially applying his learning to practical extrusion. He also holds a part-time position as Professor of Production Technology at Bournemouth University. His e-mail is: Tsheppar@bournemouth.ac.uk

Zhi Peng was born in China and now study in the University of Bournemouth, U.K. for his Ph.D's degree. His e-mail address is: Zpeng@bournemouth.ac.uk